Original Article

Diagnostic value of endobronchial ultrasound elastography in differentiating between benign and malignant hilar and mediastinal lymph nodes: a retrospective study

Yueming Wang[1,2#], Zhigang Zhao[3#], Minghui Zhu[4#], Qiang Zhu[2], Zhen Yang[2], Liangan Chen[1,2]

[1]School of Medicine, Nankai University, Tianjin, China; [2]Department of Pulmonary and Critical Care Medicine, Chinese PLA General Hospital, Beijing, China; [3]Department of Pulmonary and Critical Care Medicine, Henan Provincial People's Hospital, Zhengzhou, China; [4]Department of Pulmonary and Critical Care Medicine, Zhongnan Hospital of Wuhan University, Wuhan, China

Contributions: (I) Conception and design: Y Wang, Z Zhao, M Zhu, Z Yang, L Chen; (II) Administrative support: L Chen; (III) Provision of study materials or patients: Q Zhu, Z Yang; (IV) Collection and assembly of data: Y Wang; (V) Data analysis and interpretation: Z Zhao, M Zhu; (VI) Manuscript writing: All authors; (VII) Final approval of manuscript: All authors.

[#]These authors contributed equally to this work.

Correspondence to: Liangan Chen, MD. School of Medicine, Nankai University, 94 Weijin Road, Tianjin 300071, China; Department of Pulmonary and Critical Care Medicine, Chinese PLA General Hospital, 28 Fuxing Road, Beijing 100853, China. Email: lianganchen301@263.net; Zhen Yang, MD. Department of Pulmonary and Critical Care Medicine, Chinese PLA General Hospital, 28 Fuxing Road, Beijing 100853, China. Email: yztoogetyou@163.com.

Background: Endobronchial ultrasound-guided transbronchial needle aspiration (EBUS-TBNA) is a first-line approach for diagnosing hilar and mediastinal lymph node metastasis. Endobronchial ultrasound (EBUS) elastography is an imaging technique for describing the elasticity of intrathoracic lesions. However, the reported accuracy of EBUS elastography needs to be improved. In this study, we aimed to explore the diagnostic value of EBUS elastography for differentiating between benign and malignant hilar and mediastinal lymph nodes.

Methods: We conducted a single-center, retrospective study enrolling consecutive patients who received EBUS elastography followed by EBUS-TBNA at the Chinese PLA General Hospital from October 2015 to October 2022. The pathological results of EBUS-TBNA confirmed by 6-month follow-up were used as the gold standard. The ultrasound elastography parameters of lymph nodes included strain rate, stiff area ratio, and elasticity score, along with the conventional ultrasound characteristics such as short axis diameter, shape, margin, echogenicity distribution and intensity, and blood flow. The diagnostic performance of these parameters was compared, and conjointly analyzed using multivariate logistic regression. Bootstrapping resampling was applied for internal validation of the regression model.

Results: A total of 83 patients were enrolled with an average age of 57 years, and 66.3% of patients were male. In total, 131 lymph nodes were punctured, among which 79 (60.3%) were malignant. All the conventional ultrasound characteristics were significantly different between benign and malignant lymph nodes. All the ultrasound elastography parameters of malignant lymph nodes were markedly higher than those of benign lymph nodes. Multivariate logistic regression analysis showed that the margin, echogenicity intensity, blood flow, short axis diameter, and stiff area ratio were the main factors affecting the lymph node property. The diagnostic accuracy, sensitivity, and specificity were 91.8% [95% confidence interval (CI): 85.4–96.0%], 94.4% (95% CI: 86.4–98.5%), and 88.0% (95% CI: 75.7–95.5%), respectively. Bootstrap resampling validation showed a concordance index (C-index) of 0.949. The calibration plot indicated good agreement between the predicted and observed results.

Conclusions: EBUS elastography is a promising approach for differentiating between benign and

malignant lymph nodes. The combination of conventional EBUS and elastography can improve diagnostic efficacy, provide reliable complementary information, and guide the implementation of EBUS-TBNA more accurately.

Keywords: Endobronchial ultrasound (EBUS); elastography; lymph node metastasis; endobronchial ultrasound-guided transbronchial needle aspiration (EBUS-TBNA)

Submitted Feb 27, 2023. Accepted for publication May 23, 2023. Published online Jun 05, 2023.
doi: 10.21037/qims-23-241
View this article at: https://dx.doi.org/10.21037/qims-23-241

Introduction

Mediastinal and/or hilar lymphadenopathy are common in clinical practice, which can be secondary to various benign and malignant etiologies including sarcoidosis, tuberculosis, lymph node metastasis of lung cancer and extrapulmonary cancer, and reactive lymphadenopathy. For patients with suspected lung cancer accompanied by hilar or mediastinal lymphadenopathy, differentiating between benign and malignant lymph nodes is very important for diagnosis, staging, and subsequent treatment. Enlarged mediastinal and hilar lymph nodes can be preliminarily assessed using non-invasive imaging techniques. Computed tomography (CT) is the routine anatomic examination for mediastinal lymph node metastasis using the short-axis diameter of more than 1 cm as the criterion for lymph nodal positivity, but its sensitivity and specificity have been reported to be only 55% and 81%, respectively (1). Positron emission tomography (PET)/CT has been shown to be more accurate than CT with a sensitivity of 72% and a specificity of 91% for mediastinal nodal staging (2). A meta-analysis demonstrated that the sensitivity and specificity of magnetic resonance imaging (MRI) were 87% and 88% in staging hilar and mediastinal lymph nodes in non-small cell lung cancer (NSCLC) (3). These results indicate that there are still some false-positive and false-negative findings from noninvasive tests, and invasive methods are needed to further provide definitive tissue diagnosis for suspicious lymph nodes. Although mediastinoscopy is the traditional gold standard with high accuracy, its operation is relatively complex and difficult with potentially severe complications in some cases (4). In 2002, the Olympus Corporation (Tokyo, Japan) equipped bronchoscopes with miniature ultrasound probes, which enabled the use of real-time endobronchial ultrasound-guided transbronchial needle aspiration (EBUS-TBNA) for the biopsy of hilar and mediastinal lymph nodes (5). The sensitivity and specificity of EBUS-TBNA in detecting metastatic mediastinal lymph node in lung cancer have been reported at 93% and 100%, respectively (6). Furthermore, EBUS-TBNA has exhibited equally high diagnostic accuracy and lower complication rate in comparison with mediastinoscopy for mediastinal lymph node staging of NSCLC (7,8). In 2007, the American College of Chest Physicians (ACCP) and the National Comprehensive Cancer Network (NCCN) recommended EBUS-TBNA as an important tool for the preoperative evaluation and staging of lung cancer. EBUS-TBNA is a safe technique that can be used not only for the diagnosis and staging of lung cancer but also for the diagnosis of other benign or malignant lesions in the hilum and mediastinum (9,10). The traditional procedure of EBUS-TBNA for mediastinal and hilar lymph nodes is sequentially performed according to the lymph node stations. Therefore, accurate prediction of lymph node property before puncture is expected to improve the efficiency of biopsy, avoid procedural complications of multi-station puncture, and reduce potential risk of malignant lymph node metastasis. Conventional characteristics of targeted lymph nodes, including size, shape, margin, echogenicity, and the presence of coagulation necrosis signs can be obtained during EBUS-TBNA. Multivariate analysis revealed that round shape, distinct margin, heterogeneous echogenicity, and presence of coagulation necrosis sign were independent predictive factors for metastasis (11). However, research had shown that the accuracy of predicting lymph node properties using these features is only 63.8–86% (11). Therefore, new ultrasound techniques that improve the accuracy of EBUS-TBNA and avoid unnecessary biopsies are needed.

Elastography is a quantitative technique for imaging strain and elastic modulus distributions in soft tissues that has good resolution and sensitivity (12). Tissues respond to external or internal compression with deformation,

displacement, or velocity, and this response can be digitally transmitted and superimposed into a 2-dimensional (2D) ultrasound image that reflects the stiffness of tissues using a color-coded system, ranging from red (softest) to green (intermediate) to blue (hardest). Malignant tumors are stiffer than normal tissues and exhibit less elasticity, making it feasible for ultrasound elastography to distinguish malignant from benign lesions. Ultrasound elastography has high diagnostic value in differentiating between benign and malignant lesions in the liver, kidney, pancreas, breast, thyroid, prostate, and lymph nodes (13-21). The diagnostic utility of endobronchial ultrasound (EBUS) elastography to determine the properties of hilar and mediastinal lymph nodes was also evaluated in some studies (22-28). However, the optimal and standard evaluation method remains unclear, and the accuracy of EBUS elastography in the majority of these reported studies needs to be improved. In this study, we aimed to investigate the diagnostic value of EBUS elastography for differentiating between benign and malignant lymph nodes in the hilum and mediastinum. We sought to improve the accuracy of EBUS elastography by performing various analyses on the elastographic images. We present this article in accordance with the STARD reporting checklist (available at https://qims.amegroups.com/article/view/10.21037/qims-23-241/rc).

Methods

Patient enrollment

This single-center, retrospective study enrolled consecutive patients who underwent EBUS elastography followed by EBUS-TBNA examination at the Department of Pulmonary and Critical Care Medicine of the Chinese PLA General Hospital from October 2015 to October 2022. The inclusion criteria for patients were as follows: (I) aged 18 years or older; (II) with enlarged hilar or mediastinal lymph nodes (short axis diameter ≥1 cm) on thoracic CT scan and/or positron emission tomography-CT (PET-CT); (III) receiving conventional EBUS and EBUS elastography followed by EBUS-TBNA. In this retrospective study, diagnostic results were confirmed in the following procedures. First, the patients who obtained confirmed pathological diagnosis through EBUS-TBNA were included. Second, when EBUS-TBNA could not provide the confirmed diagnostic result, the patients who could be diagnosed by the results of other relevant clinical examinations, surgery, empirical treatment, or follow-up observation in the following 6 months after EBUS-TBNA were also included. The exclusion criteria were as follows: (I) lacking confirmed diagnostic result; (II) lost to follow-up. The study was conducted in accordance with the Declaration of Helsinki (as revised in 2013) and was approved by the Ethics Committee of the Chinese PLA General Hospital (No. S2022-762-01). The requirement for individual consent for this retrospective study was waived.

Data collection and image analysis

The demographic and clinical data of the patients were collected and recorded, including age, sex, total operation time, and the number, station, and needle passes of lymph nodes. All patients received conventional EBUS and EBUS elastography examinations followed by EBUS-TBNA. Conventional EBUS was performed using an ultrasound bronchoscope (BF-UC260; Olympus, Tokyo, Japan) with a dedicated ultrasound processor (EU-ME2 Premier Plus, Olympus). The conventional ultrasound characteristics of lymph nodes were evaluated according to the images and videos recorded intraoperatively, including B-mode ultrasound characteristics (short axis diameter, shape, margin, echogenicity distribution and intensity) and Doppler ultrasound characteristic (blood flow), which were defined based on the previous study (11) with some modifications as follows: (I) short axis diameter: the maximum transverse diameter perpendicular to the longest longitudinal diameter (long axis diameter) of the maximum cross-section of the lymph node. (II) The shape was categorized as round when the ratio of the long to short axis diameter of the lymph node was <1.5; otherwise, it was categorized as oval. (III) The margin was categorized as distinct when more than 50% of the margin between the lymph node and surrounding tissues was clearly visualized; otherwise, it was categorized as indistinct. (IV) The echogenicity distribution was categorized as homogeneous when the internal echogenicity of the lymph node was uniform; otherwise, it was categorized as heterogeneous. (V) The echogenicity intensity was categorized as hypoechoic, isoechoic, or hyperechoic based on the echogenic differences between the lymph node and the surrounding connective tissue. (VI) blood flow was evaluated on the Doppler-mode images. When there was no blood flow, or only a small amount of punctiform or short rod-shaped flow distributed in the center of the lymph node, the blood flow was categorized as poor; when there were multiple rod-shaped or aberrant long strips of flow inside or surrounding

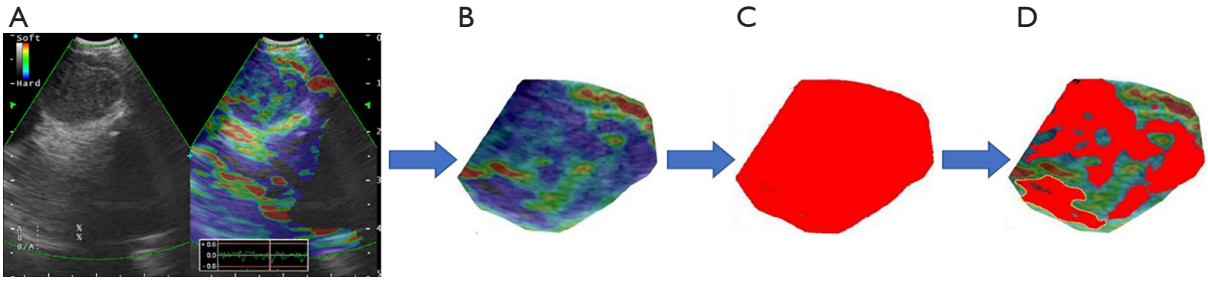

Figure 1 Quantification of the stiff area ratio of representative elastographic images by ImageJ software. The image of targeted lymph node area (B) was selected based on the B-mode image (A), and the pixels of the whole lymph node area (C) were measured. We adjusted the hue [145–180] and brightness [0–255] of the image to measure the pixels of the relatively stiffer tissue area (blue pixel area) (D). The stiff area ratio was defined as the ratio of the pixels of the stiffer tissue area to the whole lymph node area.

the lymph node, the blood flow was categorized as rich.

Next, the lymph nodes were observed with EBUS elastography. An elastographic image was obtained using the "freeze" function, and the frame with the highest frequency of image features was selected with the trackball to measure the strain ratio. The same elastographic image was then used to determine the stiff area ratio and elasticity score. The parameters analyzed were defined as follows:

(I) Strain ratio: the ratio of the strain rate of the surrounding normal tissue (red and green areas) to the whole lymph node was the average strain ratio; the ratio of the strain rate of surrounding normal tissue to the hardest area (blue area) of the lymph node was the maximum strain ratio; the ratio of strain rate of surrounding normal tissue to the softest area (red area) of the lymph node was the minimum strain ratio.

(II) The elasticity score was determined using a semiquantitative 4-point scale for lymph node elastography, as previously reported (23). Images with red and green areas accounting for more than 80% were marked as 1 point; images with red and green areas accounting for 50–80% were marked as 2 points; images with the blue area accounting for 50–80% were marked as 3 points; images with the blue area accounting for more than 80% were marked as 4 points.

(III) The stiff area ratio was calculated by ImageJ software, version 1.6.0 (National Institutes of Health, Bethesda, MD, USA), as shown in *Figure 1*. The elastographic image was imported into ImageJ software, and the image of the targeted lymph node was cut to calculate the pixels of the whole lymph node area. Next, the hue value was adjusted to 145–180 (blue) and the brightness value was adjusted to 0–255 to calculate the pixels of the relatively stiffer tissue area (blue area). The stiff area ratio was defined as the ratio of the pixels of the stiffer tissue area to the whole lymph node area.

EBUS-TBNA was performed with the 22G puncture needle (NA-201SX-4022, Olympus). The obtained tissues and puncture fluid smear were sent to the Department of Pathology for routine histological and cytological analysis. The pathological results of the specimens obtained by EBUS-TBNA were used as the gold standard, and benign disease was confirmed by follow-up in the following 6 months after EBUS-TBNA. The conventional ultrasound characteristics and ultrasound elastography parameters were assessed by 2 investigators, one with more than 5 years' work experience in ultrasonic diagnosis and the other with more than 5 years' work experience in endobronchial ultrasonography, who were blinded to the clinical data and pathological results of patients.

Statistical analysis

Normally distributed quantitative data were exhibited as the mean ± standard deviation (SD) and compared using Student's *t*-test. Non-normally distributed quantitative data were expressed as the median and range and compared using the Wilcoxon rank-sum test. Categorical data were shown as a percentage and were compared by the chi-square test.

A receiver operating characteristic (ROC) curve was built to obtain the area under the ROC curve (AUC) that was compared using Z test. For ultrasound elastography

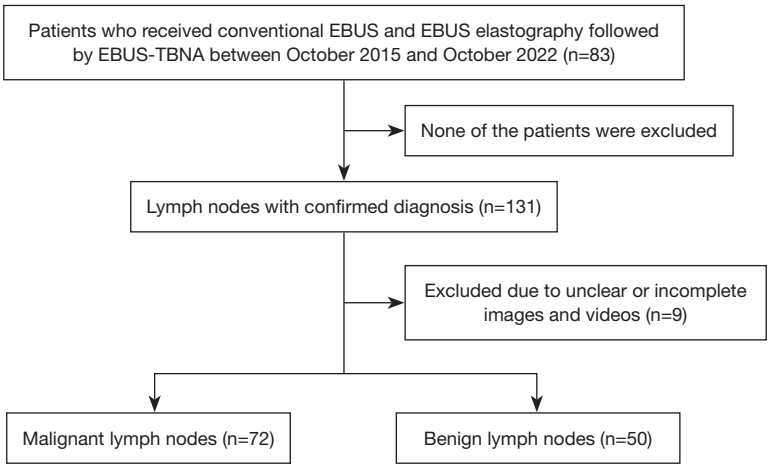

Figure 2 Flow chart for the inclusion and exclusion of the patients and lymph nodes. EBUS, endobronchial ultrasound; EBUS-TBNA, endobronchial ultrasound-guided transbronchial needle aspiration.

parameters, the maximum Youden index (sensitivity + specificity −1) was used to identify the optimal cutoff value on the ROC curve. Accuracy, sensitivity, specificity, positive predictive value (PPV), and negative predictive value (NPV) of ultrasound elastography parameters were calculated based on the cutoff value. The accuracy was compared using the chi-square test. Multivariate analysis was performed using binary logistic regression, which included the conventional ultrasound characteristics and ultrasound elastography parameters with P values less than 0.05 in the univariate analysis. The likelihood ratio test was used for fitting the multivariate logistic regression model. Internal validation of the model was performed using bootstrap resampling (1,000 bootstrap resamples), and the calibration curve was plotted to evaluate the calibration of the model. Interobserver agreement was evaluated by Kappa (κ) analysis. Statistical analyses were carried out using the software SPSS 17.0 (IBM Corp., Chicago, IL, USA) and R software, version 4.2.2 (The Free Software Foundation, Boston, MA, USA). A 2-sided P value less than 0.05 was considered statistically significant.

Results

Characteristics of the patients and lymph nodes

As shown in *Figure 2* and *Table 1*, a total of 83 patients (55 males and 28 females) were enrolled in this study, with an average age of 57 years (range, 31–84 years). We punctured 131 lymph nodes with 381 total needle passes, and the average operation time for each patient was 43±15 minutes. The detailed distribution of lymph node stations was as follows: station 2 (3, 2.3%), station 4R (38, 29.0%), station 4L (10, 7.6%), station 7 (41, 31.3%), station 10R (5, 3.8%), station 11R (18, 13.7%), and station 11L (16, 12.2%). Among the 131 lymph nodes punctured through EBUS/TBNA, the pathological results of 73 lymph nodes (55.7%) were malignant. The other 58 lymph nodes (44.3%) were pathologically benign, among which 6 lymph nodes were confirmed to be malignant through other relevant clinical examinations, surgery, or empirical treatment during 6-month follow-up. The sensitivity, specificity, and accuracy of EBUS-TBNA were 92.4% [95% confidence interval (CI): 84.2–97.2%], 100% (95% CI: 93.2–100%), and 95.4% (95% CI: 90.3–98.3%), respectively. The final diagnoses of the lymph nodes are shown in *Table 1*.

Comparison of conventional ultrasound characteristics and ultrasound elastography parameters between benign and malignant lymph nodes

Among the 131 lymph nodes, 9 were excluded from the analysis of conventional ultrasound characteristics and ultrasound elastography parameters because the recorded images and videos were unclear or incomplete. The interobserver agreement for the shape, margin, echogenicity distribution and intensity, blood flow, and elasticity score was excellent with κ values of 0.947 (P<0.001), 0.892 (P<0.001), 0.857 (P<0.001), 0.853 (P<0.001), 0.918 (P<0.001), and 0.892 (P<0.001), respectively. As shown in *Table 2*, the conventional ultrasound characteristics, including shape,

Table 1 Baseline characteristics of patients and lymph nodes

Characteristics	Numbers
Gender, n (%)	
Male	55 (66.3)
Female	28 (33.7)
Age, years, average [range]	57 [31–84]
Operation time per patient, minutes, average ± SD	43±15
Total needle passes, n	381
Total lymph nodes, n	131
Final diagnosis, n (%)	
Malignant	
Adenocarcinoma	31 (23.7)
Squamous cell carcinoma	13 (9.9)
Small cell carcinoma	26 (19.8)
Poorly differentiated carcinoma	6 (4.6)
Malignant mesothelioma	1 (0.8)
Metastatic renal cell carcinoma	1 (0.8)
Metastatic intestinal cancer	1 (0.8)
Benign	
Tuberculosis	14 (10.7)
Sarcoidosis	13 (9.9)
Undefined granuloma	12 (9.2)
Reactive lymph node hyperplasia	12 (9.2)
Other	1 (0.8)

n, number; SD, standard deviation.

margin, echogenicity distribution and intensity, and blood flow, were significantly different between the benign and malignant lymph nodes. Round shape, distinct margin, heterogeneous and hypoechoic echogenicity, and rich blood flow were more common in malignant lymph nodes. Also, the diameters of malignant lymph nodes were significantly longer than those of benign lymph nodes. We also compared the differences in ultrasound elastography parameters, such as strain ratio, stiff area ratio, and elasticity score, between benign and malignant lymph nodes (*Table 2*). The average, maximum, and minimum strain ratios of malignant lymph nodes were markedly higher than those of benign lymph nodes. In addition, the stiff area ratios and elasticity scores of malignant lymph nodes were also considerably higher than those of benign lymph nodes.

Diagnostic value of conventional ultrasound characteristics and ultrasound elastography parameters in differentiating between benign and malignant lymph nodes

The pathological results of the specimens obtained by EBUS-TBNA were used as the gold standard. The ROC curves of conventional ultrasound characteristics are shown in *Figure 3A*. The AUC of each characteristic was compared with AUC =0.5, and all the differences were statistically significant, indicating that shape, margin, echogenicity distribution and intensity, and blood flow of lymph nodes had diagnostic value for the differentiation between benign and malignant lymph nodes. The accuracy, sensitivity, specificity, PPV, and NPV of ultrasound characteristics were calculated and are shown in *Table 3*.

The ROC curves of different ultrasound elastography parameters are presented in *Figure 3B*, and the AUC values were also compared with AUC =0.5. The results showed that the average strain ratio, stiff area ratio, and elasticity score had notable diagnostic value for differentiating between benign and malignant lymph nodes. The optimal cutoff values for the average strain ratio, maximum strain ratio, minimum strain ratio, stiff area ratio, and elasticity score were 14.33, 117.84, 2.28, 0.60, and 2.5, respectively. The accuracy, sensitivity, specificity, PPV, and NPV of each ultrasound elastography parameter were also calculated and are shown in *Table 3*.

The accuracy of the average strain ratio, stiff area ratio, and elasticity score in the differential diagnosis of benign and malignant lymph nodes was 82.0% (95% CI: 74.0–88.3%), 84.4% (95% CI: 76.8–90.4%), and 83.6% (95% CI: 75.8–89.7%), respectively, and the AUCs were 0.882 (95% CI: 0.822–0.942), 0.875 (95% CI: 0.808–0.942), and 0.837 (95% CI: 0.759–0.914), respectively. There were no significant differences in the accuracy and AUC among the 3 elastography parameters. We then compared the accuracy and AUCs of ultrasound elastography parameters with the conventional ultrasound characteristics (*Table 3*). We found that the accuracy of the average strain ratio was significantly higher than that of the shape (P=0.002), margin (P=0.035), echogenicity distribution (P=0.004), maximum strain ratio (P=0.008), and minimum strain ratio (P=0.025). The accuracy of the stiff area ratio was significantly higher than that of the shape (P<0.001), margin (P=0.009), echogenicity distribution (P=0.001), echogenicity intensity (P=0.041), blood flow (P=0.02), maximum strain ratio (P=0.002), and minimum strain ratio (P=0.006). The accuracy of the elasticity score was significantly higher than that of

Table 2 Comparison of the conventional ultrasound characteristics and ultrasound elastography parameters between benign and malignant lymph nodes

Variables	Benign LNs (n=50)	Malignant LNs (n=72)	P value
Conventional ultrasound characteristics			
Shape			
Round	20 (40.0)	49 (68.1)	0.002**
Oval	30 (60.0)	23 (31.9)	
Margin			
Distinct	21 (42.0)	51 (70.8)	0.001**
Indistinct	29 (58.0)	21 (29.2)	
Echogenicity			
Heterogeneous	20 (40.0)	50 (69.4)	0.001**
Homogeneous	30 (60.0)	22 (30.6)	
Echogenicity			
Hypoechoic	16 (32.0)	56 (77.8)	<0.001***
Iso- or hyper-echoic	34 (68.0)	16 (22.2)	
Blood flow			
Rich	7 (14.0)	45 (62.5)	<0.001***
Poor	43 (86.0)	27 (37.5)	
Short axis diameter, mm	17.0 (8.1, 45.5)	23.5 (10.4, 61.7)	<0.001***
Ultrasound elastography parameters			
Average strain ratio	5.12 (0.21, 35.20)	25.57 (2.37, 245.67)	<0.001***
Maximum strain ratio	75.53±48.28	127.57±69.98	<0.001***
Minimum strain ratio	1.51 (0.10, 11.31)	3.57 (0.37, 77.33)	<0.001***
Stiff area ratio	0.42 (0.11, 0.88)	0.72 (0.12, 0.97)	<0.001***
Elasticity score			<0.001***
1	13 (26.0)	2 (2.8)	
2	25 (50.0)	6 (8.3)	
3	9 (18.0)	43 (59.7)	
4	3 (6.0)	21 (29.2)	

Data are presented as n (%), median (range), or mean ± SD. **, P<0.01; ***, P<0.001. LN, lymph node; SD, standard deviation.

the shape (P=0.001), margin (P=0.015), echogenicity distribution (P=0.001), blood flow (P=0.031), maximum strain ratio (P=0.003), and minimum strain ratio (P=0.01). The AUC of the average strain ratio was significantly higher than that of the shape (P<0.001), margin (P<0.001), echogenicity distribution (P<0.001), echogenicity intensity (P=0.007), blood flow (P=0.010), maximum strain ratio (P=0.004), and minimum strain ratio (P=0.003). The AUC of the stiff area ratio was significantly higher than that of the shape (P<0.001), margin (P<0.001), echogenicity distribution (P<0.001), echogenicity intensity (P=0.013), blood flow (P=0.018), maximum strain ratio (P=0.008), and minimum strain ratio (P=0.006). The AUC of the elasticity score was significantly higher than that of the shape

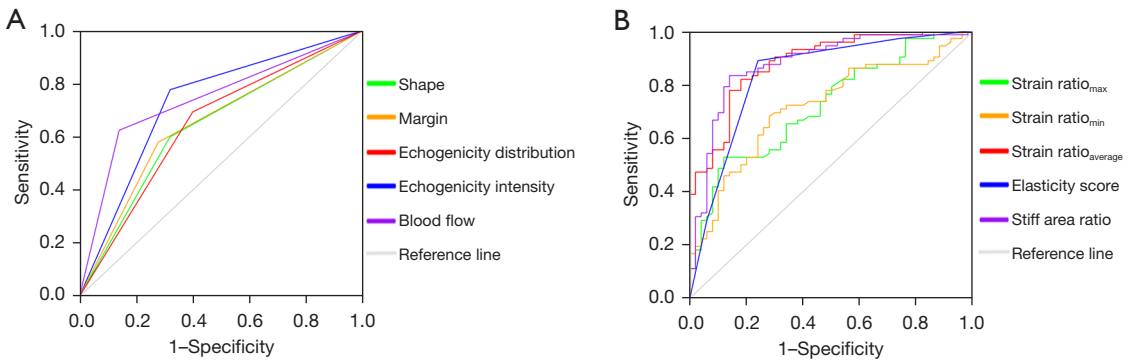

Figure 3 ROC curves of the conventional ultrasound characteristics (A) and ultrasound elastography parameters (B) in differentiating between benign and malignant lymph nodes. Strain ratio$_{max}$, maximum strain ratio; Strain ratio$_{min}$, minimum strain ratio; Strain ratio$_{average}$, average strain ratio; ROC, receiver operating characteristic.

Table 3 Diagnostic performance of conventional ultrasound characteristics and ultrasound elastography parameters in differentiating between benign and malignant lymph nodes

Variables	Accuracy (%)	Sensitivity (%)	Specificity (%)	PPV (%)	NPV (%)	AUC (95% CI)
Conventional ultrasound characteristics						
Round shape	64.8†‡§	68.1	60.0	71.0	56.6	0.640 (0.539–0.741)†‡§
Distinct margin	70.5†‡§	72.2	58.0	76.5	63.0	0.651 (0.551–0.752)†‡§
Heterogeneous echogenicity	65.6†‡§	69.4	60.0	71.4	57.7	0.647 (0.547–0.748)†‡§
Hypoechoic echogenicity	73.8‡	77.8	68.0	77.8	68.0	0.729 (0.635–0.823)†‡
Rich blood flow	72.1‡§	62.5	86.0	86.5	61.4	0.742 (0.654–0.831)†‡
Ultrasound elastography parameters						
Average strain ratio	82.0	81.9	82.0	86.8	75.9	0.882 (0.822–0.942)
Maximum strain ratio	67.2†‡§	52.8	88.0	86.4	56.4	0.724 (0.634–0.813)†‡
Minimum strain ratio	69.7†‡§	68.1	72.0	77.8	61.0	0.719 (0.628–0.810)†‡
Stiff area ratio	84.4	83.3	86.0	89.6	78.2	0.875 (0.808–0.942)
Elasticity score	83.6	88.9	76.0	84.2	82.6	0.837 (0.759–0.914)

†, P<0.05 compared with the average strain ratio; ‡, P<0.05 compared with the stiff area ratio; §, P<0.05 compared with the elasticity score. PPV, positive predictive value; NPV, negative predictive value; AUC, area under the curve; CI, confidence interval.

(P=0.002), margin (P=0.004), and echogenicity distribution (P=0.003).

Diagnostic value of the stiff area ratio and strain ratio in differentiating between benign and malignant lymph nodes at different lymph node stations

The deformation of lymph nodes at different stations may differ due to the different degrees of compression they experience, which may produce different elastographic images for lymph nodes with the same properties. In this study, we further analyzed the diagnostic value of the stiff area ratio and average strain ratio for distinguishing benign from malignant lymph nodes at different stations (*Table 4*). Using the station-specific cutoff values of the stiff area ratio, the accuracy, sensitivity, and specificity were 90.1% (95% CI: 83.6–94.6%), 89.9% (95% CI: 81–95.5%), and 90.4% (95% CI: 79.0–96.8%), respectively, which were higher than those shown above when using 0.6 as the unified cutoff value. However, the differences were not statistically

Table 4 Diagnostic performance of the stiff area ratio and average strain ratio for differentiation of benign and malignant lymph nodes at different stations

LN station	Elastography parameters	Cutoff value	Accuracy (%)	Sensitivity (%)	Specificity (%)
2R	Stiff area ratio	0.52	–	–	–
	Average strain ratio	8.44	–	–	–
4R	Stiff area ratio	0.60	92.1	92.0	92.3
	Average strain ratio	15.43	83.8	83.3	84.6
4L	Stiff area ratio	0.30	100	100	100
	Average strain ratio	2.40	100	100	100
7	Stiff area ratio	0.64	82.9	82.6	83.3
	Average strain ratio	14.86	76.3	77.3	75.0
10R	Stiff area ratio	0.43	–	–	–
	Average strain ratio	14.33	–	–	–
11R	Stiff area ratio	0.57	83.3	80.0	87.5
	Average strain ratio	11.51	82.4	77.8	87.5
11L	Stiff area ratio	0.69	100	100	100
	Average strain ratio	17.29	100	100	100

LN, lymph node; R, right; L, left.

significant.

We then utilized the same method to analyze the diagnostic value of the average strain ratio at different lymph node stations (*Table 4*). With the station-specific cutoff values of the average strain ratio, the accuracy, sensitivity, and specificity were 85.3% (95% CI: 77.7–91.0%), 84.7% (95% CI: 74.3–92.1%), and 86.0% (95% CI: 73.3–94.2%), which were also higher than those shown above when using 14.33 as the unified cutoff value. However, the differences were not statistically significant.

Combination of conventional ultrasound characteristics and ultrasound elastography parameters for the diagnosis of benign and malignant lymph nodes

We constructed a multivariate logistic regression model, taking the pathological results of lymph nodes as the dependent variable and the above conventional ultrasound characteristics and ultrasound elastography parameters as independent variables. Regression analysis showed that the main factors affecting the property of lymph nodes were margin, echogenicity intensity, blood flow, short axis diameter, and stiff area ratio (*Table 5*). The likelihood ratio test was performed (χ^2=98.992, P=0.000), which showed that the regression model was statistically significant. The ROC curve was drawn (*Figure 4*), and the AUC was 0.949 (95% CI: 0.911–0.988). The diagnostic results of the lymph nodes made by the multivariate logistic regression model and the reference standard are shown in *Table 6*. The diagnostic accuracy, sensitivity, and specificity were 91.8% (95% CI: 85.4–96.0%), 94.4% (95% CI: 86.4–98.5%), and 88.0% (95% CI: 75.7–95.5%), respectively, indicating that the model had a high diagnostic value. The accuracy and AUC of the regression model were higher than those of the above-mentioned conventional ultrasound characteristics and ultrasound elastography parameters, and the differences were statistically significant. We conducted internal validation of the model by bootstrapping with 1,000 resamples, which showed a concordance index (C-index) of 0.949. The calibration plot indicated good agreement between the predicted and observed results (*Figure 5*).

Discussion

Determining whether enlarged hilar and mediastinal lymph nodes are malignant is critical for the diagnosis, staging, treatment, and prognostic evaluation of lung cancer. EBUS-TBNA is considered a top-choice diagnostic procedure for

Table 5 Results of significant factors by multivariate logistic regression analysis

Variables	Regression coefficient	Standard error	P value	OR	95% CI
Margin	1.418	0.644	0.028*	0.242	0.068–0.856
Echogenicity intensity	2.102	0.687	0.002**	8.183	2.128–31.476
Blood flow	2.388	0.754	0.002**	10.896	2.487–47.734
Short axis diameter	0.077	0.033	0.020*	1.080	1.012–1.152
Stiff area ratio	7.592	1.787	<0.001***	1,981.381	59.633–65,833.830
Constant	–7.043	1.517	<0.001***	0.001	–

*, P<0.05; **, P<0.01; ***, P<0.001. OR, odds ratio; CI, confidence interval.

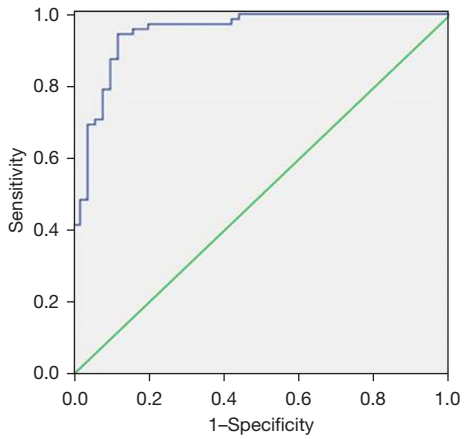

Figure 4 ROC curve of the multivariate logistic regression model in differentiating between benign and malignant lymph nodes. ROC, receiver operating characteristic.

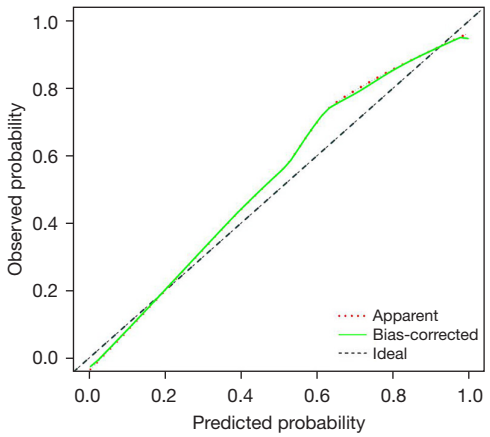

Figure 5 The calibration curve of internal validation by bootstrapping resampling (1,000 bootstrap resamples) method.

Table 6 The diagnostic results of the lymph nodes made by the multivariate logistic regression model and the reference standard

Multivariate logistic regression model	Gold standard		
	Malignant	Benign	Total
Malignant	68	6	74
Benign	4	44	48
Total	72	50	122

confirming the presence of lymph node metastasis due to its minimal invasiveness and high accuracy (29). Before EBUS-TBNA, it is important to preliminarily determine the properties of targeted lymph nodes based on the ultrasound characteristics, so that the puncture can be conducted accordingly. With the rapid development of ultrasound technology, ultrasound elastography has been gradually applied in clinical practice, especially in breast and thyroid diseases (17,18). EBUS elastography is also promising for the differentiation of benign and malignant lymph nodes.

In this study, we analyzed the utility of conventional ultrasound characteristics in differentiating between benign and malignant hilar and mediastinal lymph nodes. The results showed that there were significant differences in the distribution of conventional ultrasound characteristics, including lymph node shape, margin, echogenicity distribution and intensity, and blood flow, between benign and malignant lymph nodes. When these characteristics were used for differentiating between benign and malignant lymph nodes, the accuracy ranged from 64.8% to 73.8%, and the AUC ranged from 0.640 to 0.742, indicating a relatively low diagnostic value, which was consistent with previous research (11).

EBUS elastography can be evaluated through qualitative

and quantitative techniques. The qualitative methods include elastographic patterns (3 image types) (22), and 4-point (23) and 5-point (24) elasticity score systems, which are mainly based on the color distribution of the elastographic images. The most frequently reported method is the 3-image pattern classification (22): type 1, predominantly non-blue (green, yellow, and red); type 2, part blue, part non-blue (green, yellow, and red); type 3, predominantly blue. However, there is a major drawback that the type 2 is equivocal. In this study, we selected the elasticity score (4-point scale) as the qualitative evaluation parameter. The results showed that the elasticity score of malignant lymph nodes was markedly higher than that of benign lymph nodes. With an optimal cutoff value of 2.5, the accuracy, sensitivity, and specificity of the elasticity score were 83.6% (95% CI: 75.8–89.7%), 88.9% (95% CI: 79.3–95.1%), and 76% (95% CI: 61.8–86.9%), respectively, and the AUC was 0.837 (95% CI: 0.759–0.914). He *et al.* (23) used the same scoring system, and the accuracy, sensitivity, and specificity of their study were 82.3%, 76.9%, and 85.7%, respectively, with the cutoff value of 2.5. In another similar study (30), the accuracy, sensitivity, and specificity were only 68%, 79%, and 60%, respectively, with the cutoff value of 3. The differences in cutoff value and diagnostic efficacy might be mainly attributed to the subjective factors of the investigators.

The quantitative parameters of EBUS elastography assessment mainly include the strain ratio, stiff area ratio, blue color proportion, and strain histogram. The most frequently reported quantitative method is the measurement of the strain ratio, which can be performed in real time with relatively simple operation (25). In this study, we found that the strain ratio of malignant lymph nodes was markedly higher than that of benign lymph nodes. With an optimal cutoff value of 14.33, the accuracy, sensitivity, and specificity of the average strain ratio in our study were 82.0% (95% CI: 74.0–88.3%), 81.9% (95% CI: 71.1–90.0%), and 82.0% (95% CI: 68.6–91.4%), respectively, and the AUC was 0.882 (95% CI: 0.822–0.942), which were significantly higher than the diagnostic values of conventional ultrasound characteristics. The cutoff value of the strain ratio in our study differed from the values reported in the previous studies that ranged from 2.47 to 32.07 (23,25,28,30,31), which may be related to the differences in equipment, and limited uniformity of the surrounding tissues selected for calculation by the investigators. We also calculated the stiff area ratio of the lymph nodes using Image J software, which could objectively evaluate the stiffness of the whole lymph node (26). The stiff area ratio of malignant lymph nodes was significantly higher than that of benign lymph nodes (0.72 *vs.* 0.42). With an optimal cutoff value of 0.6, the accuracy, sensitivity, and specificity of the stiff area ratio were 84.4% (95% CI: 76.8–90.4%), 83.3% (95% CI: 72.7–91.1%), and 86.0% (95% CI: 73.3–94.2%), respectively, and the AUC was 0.875 (95% CI: 0.808–0.942), which were also significantly higher than those of conventional ultrasound characteristics. The cutoff value of the stiff area ratio was higher than the values (0.311–0.52) of other studies, but the diagnostic values were similar (26,32-35). The higher cutoff value may result from the relatively higher percentage of patients with tuberculosis that was associated with hardened lymph nodes, indicating that the medical history of patients may affect the results of EBUS elastography (34). Ma *et al.* (27) measured the blue color proportion of lymph nodes with the similar principle of strain area ratio, which was calculated through dividing the pixel value of the blue area by the pixel value of the whole lymph node using the Photoshop software (Adobe, San Jose, CA, USA). Although the sensitivity reached 92.3%, the specificity and accuracy were only 67.5% and 78.5%, respectively. There were other studies using the strain histogram as the quantitative method. The strain histogram method can calculate the mean gray value of the lymph node through a software developed by MATLAB (MathWorks, Natick, MA, USA) that transforms the image from the 3 principal components of red-green-blue color to gray scale, in which these values vary from 255 (all blue pixels) to 0 (all red pixels) (24). The cutoff values of mean gray value were different between the reported studies, and the diagnostic specificity was relatively low (24,36). Collectively, the diagnostic cutoff value, accuracy, sensitivity, and specificity of ultrasound elastography parameters in our study varied from those reported in other studies to some extent, which might be attributed to the sample size, equipment, image selection standards, medical history of patients, and subjective factors of the operators. Therefore, multicenter studies with larger sample sizes are needed, and a standard evaluation system should be constructed to improve the application value of EBUS elastography.

The generation of elastographic images of enlarged hilar and mediastinal lymph nodes depends on physiological activities such as vascular pulsation, respiratory movement, and heart beating. The deformation of lymph nodes at different stations is induced by different degrees of compression, and thus, there may be differences in the elastographic images of lymph nodes with the same properties. To evaluate the diagnostic value of ultrasound

elastography for hilar and mediastinal lymph nodes more accurately, we further selected 2 relatively objective parameters (i.e., stiff area ratio and average strain ratio) to evaluate their diagnostic performance according to the location of the lymph nodes. Lymph nodes at different stations were evaluated as benign or malignant based on their respective cutoff values, which could correct some cases of missed diagnosis and exclude cases of misdiagnosis before grouping by station. For example, the lymph nodes at station 2R were all malignant, and the minimum stiff area ratio was 0.52, which was lower than that of the overall lymph nodes studied (0.6). Therefore, diagnosis based on the overall cutoff value will lead to false negative cases. Similarly, the cutoff values of stiff area ratio at station 4L and 11R were lower than 0.6, with which some false negative cases diagnosed based on the overall cutoff value could be corrected. On the contrary, the cutoff values of stiff area ratio at station 7 and 11L were higher than 0.6, with which some false positive cases could be excluded. The accuracy, sensitivity, and specificity of the stiff area ratio after grouping by station were 90.1% (95% CI: 83.6–94.6%), 89.9% (95% CI: 81–95.5%), and 90.4% (95% CI: 79.0–96.8%), respectively, which were higher than those determined using 0.6 as the unified cutoff value. Although the difference was not statistically significant, the diagnostic efficacy increased to some extent. Similarly, the accuracy, sensitivity, and specificity of the strain ratio after grouping by station were also higher than those determined using 14.33 as the unified cutoff value, achieving 85.3% (95% CI: 77.7–91.0%), 84.7% (95% CI: 74.3–92.1%), and 86.0% (95% CI: 73.3–94.2%), respectively. The main disadvantage of this method was that the number of lymph nodes at each station was small, which may decrease the reliability of the results. Therefore, studies with larger sample sizes are still needed to further verify the above results.

The ultrasound elastography parameters mainly reflect the stiffness of the tissue. However, when there is exudation, necrosis, or hemorrhage in the malignant lymph node, the stiffness of tissues can decrease, which may lead to reduction of the strain ratio, stiff area ratio, and elasticity score of lymph nodes, resulting in missed diagnosis. On the contrary, when fibrinoid material, carbon deposition, or epithelioid cell infiltration is present in benign lymph nodes, tissue stiffness will increase, which may lead to an increase in the strain ratio, stiff area ratio, and elasticity score of lymph nodes, resulting in misdiagnosis. In this study, the conventional ultrasound characteristics and ultrasound elastography parameters were jointly analyzed to construct a logistic regression model. The accuracy, sensitivity, and specificity of the model were 91.8% (95% CI: 85.4–96.0%), 94.4% (95% CI: 86.4–98.5%), and 88.0% (95% CI: 75.7–95.5%), respectively, and the AUC was 0.949 (95% CI: 0.911–0.988), which were significantly higher than those of the conventional ultrasound characteristics and ultrasound elastography parameters alone. As the sample size was not big enough to properly set training and validation groups, we performed internal validation of the multiple regression model by bootstrapping with 1,000 resamples, which showed a high C-index of 0.949 and an acceptable calibration capability. In addition, EBUS elastography has not been widely used in clinical practice, making it difficult to conduct geographically external validation in other hospitals. We intend to collect more cases in our hospital to develop a temporal validation cohort in the future.

There were some limitations in this study. First, this was a single-center retrospective study, which may have led to potential selection bias. Second, the sample size was not big enough to properly set training and validation groups, so we performed internal validation by bootstrapping with 1,000 resamples. Multicenter, prospective research is needed to perform external validation to further confirm the reliability of the model. Third, although we innovatively evaluated the property of lymph nodes using strain ratio and stiff area ratio with their respective cutoff values at different stations, the relatively small sample size at each station may decrease the reliability of the results. Therefore, studies with larger sample sizes are still needed to further verify the above results.

Conclusions

In conclusion, the present study showed that the diagnostic value of EBUS elastography parameters for differentiating between hilar and mediastinal lymph nodes was higher than that of the conventional ultrasound characteristics. Furthermore, the combined application of conventional EBUS and EBUS elastography could improve the accuracy. In clinical practice, conventional ultrasound and EBUS elastography can be combined to preliminarily determine the lesions that need to be punctured and the puncture sequence, which can guide the implementation of EBUS-TBNA more accurately.

Acknowledgments

Funding: None.

Footnote

Reporting Checklist: The authors have completed the STARD reporting checklist. Available at https://qims.amegroups.com/article/view/10.21037/qims-23-241/rc

Conflicts of Interest: All authors have completed the ICMJE uniform disclosure form (available at https://qims.amegroups.com/article/view/10.21037/qims-23-241/coif). The authors have no conflicts of interest to declare.

Ethical Statement: The authors are accountable for all aspects of the work in ensuring that questions related to the accuracy or integrity of any part of the work are appropriately investigated and resolved. This study was conducted in accordance with the Declaration of Helsinki (as revised in 2013) and was approved by the Ethics Committee of the Chinese PLA General Hospital (No. S2022-762-01). The requirement for individual consent for this retrospective study was waived.

References

1. Silvestri GA, Gonzalez AV, Jantz MA, Margolis ML, Gould MK, Tanoue LT, Harris LJ, Detterbeck FC. Methods for staging non-small cell lung cancer: Diagnosis and management of lung cancer, 3rd ed: American College of Chest Physicians evidence-based clinical practice guidelines. Chest 2013;143:e211S-50S.
2. Wu Y, Li P, Zhang H, Shi Y, Wu H, Zhang J, Qian Y, Li C, Yang J. Diagnostic value of fluorine 18 fluorodeoxyglucose positron emission tomography/computed tomography for the detection of metastases in non-small-cell lung cancer patients. Int J Cancer 2013;132:E37-47.
3. Peerlings J, Troost EG, Nelemans PJ, Cobben DC, de Boer JC, Hoffmann AL, Beets-Tan RG. The Diagnostic Value of MR Imaging in Determining the Lymph Node Status of Patients with Non-Small Cell Lung Cancer: A Meta-Analysis. Radiology 2016;281:86-98.
4. Czarnecka-Kujawa K, Yasufuku K. The role of endobronchial ultrasound versus mediastinoscopy for non-small cell lung cancer. J Thorac Dis 2017;9:S83-97.
5. Yasufuku K, Chiyo M, Sekine Y, Chhajed PN, Shibuya K, Iizasa T, Fujisawa T. Real-time endobronchial ultrasound-guided transbronchial needle aspiration of mediastinal and hilar lymph nodes. Chest 2004;126:122-8.
6. Gu P, Zhao YZ, Jiang LY, Zhang W, Xin Y, Han BH. Endobronchial ultrasound-guided transbronchial needle aspiration for staging of lung cancer: a systematic review and meta-analysis. Eur J Cancer 2009;45:1389-96.
7. Ge X, Guan W, Han F, Guo X, Jin Z. Comparison of Endobronchial Ultrasound-Guided Fine Needle Aspiration and Video-Assisted Mediastinoscopy for Mediastinal Staging of Lung Cancer. Lung 2015;193:757-66.
8. Sehgal IS, Dhooria S, Aggarwal AN, Behera D, Agarwal R. Endosonography Versus Mediastinoscopy in Mediastinal Staging of Lung Cancer: Systematic Review and Meta-Analysis. Ann Thorac Surg 2016;102:1747-55.
9. Medford AR, Bennett JA, Free CM, Agrawal S. Endobronchial ultrasound-guided transbronchial needle aspiration (EBUS-TBNA): applications in chest disease. Respirology 2010;15:71-9.
10. Sakairi Y, Nakajima T, Yoshino I. Role of endobronchial ultrasound-guided transbronchial needle aspiration in lung cancer management. Expert Rev Respir Med 2019;13:863-70.
11. Fujiwara T, Yasufuku K, Nakajima T, Chiyo M, Yoshida S, Suzuki M, Shibuya K, Hiroshima K, Nakatani Y, Yoshino I. The utility of sonographic features during endobronchial ultrasound-guided transbronchial needle aspiration for lymph node staging in patients with lung cancer: a standard endobronchial ultrasound image classification system. Chest 2010;138:641-7.
12. Ophir J, Céspedes I, Ponnekanti H, Yazdi Y, Li X. Elastography: a quantitative method for imaging the elasticity of biological tissues. Ultrason Imaging 1991;13:111-34.
13. Sigrist RMS, Liau J, Kaffas AE, Chammas MC, Willmann JK. Ultrasound Elastography: Review of Techniques and Clinical Applications. Theranostics 2017;7:1303-29.
14. Kennedy P, Wagner M, Castéra L, Hong CW, Johnson CL, Sirlin CB, Taouli B. Quantitative Elastography Methods in Liver Disease: Current Evidence and Future Directions. Radiology 2018;286:738-63.
15. Roussel E, Campi R, Amparore D, Bertolo R, Carbonara U, Erdem S, Ingels A, Kara Ö, Marandino L, Marchioni M,

Muselaers S, Pavan N, Pecoraro A, Beuselinck B, Pedrosa I, Fetzer D, Albersen M, On Behalf Of The European Association Of Urology Eau Young Academic Urologists Yau Renal Cancer Working Group. Expanding the Role of Ultrasound for the Characterization of Renal Masses. J Clin Med 2022.
16. Conti CB, Mulinacci G, Salerno R, Dinelli ME, Grassia R. Applications of endoscopic ultrasound elastography in pancreatic diseases: From literature to real life. World J Gastroenterol 2022;28:909-17.
17. Guo R, Lu G, Qin B, Fei B. Ultrasound Imaging Technologies for Breast Cancer Detection and Management: A Review. Ultrasound Med Biol 2018;44:37-70.
18. Yang K, Ye X, Tian H, Li Q, Liu Q, Li J, Guo J, Xu J, Dong F. Development and validation of a nomogram for discriminating between benign and malignant breast masses by conventional ultrasound and dual-mode elastography: a multicenter study. Quant Imaging Med Surg 2023;13:865-77.
19. Swan KZ, Nielsen VE, Bonnema SJ. Evaluation of thyroid nodules by shear wave elastography: a review of current knowledge. J Endocrinol Invest 2021;44:2043-56.
20. Anbarasan T, Wei C, Bamber JC, Barr RG, Nabi G. Characterisation of Prostate Lesions Using Transrectal Shear Wave Elastography (SWE) Ultrasound Imaging: A Systematic Review. Cancers (Basel) 2021;13:122.
21. Wang B, Guo Q, Wang JY, Yu Y, Yi AJ, Cui XW, Dietrich CF. Ultrasound Elastography for the Evaluation of Lymph Nodes. Front Oncol 2021;11:714660.
22. Izumo T, Sasada S, Chavez C, Matsumoto Y, Tsuchida T. Endobronchial ultrasound elastography in the diagnosis of mediastinal and hilar lymph nodes. Jpn J Clin Oncol 2014;44:956-62.
23. He HY, Huang M, Zhu J, Ma H, Lyu XD. Endobronchial Ultrasound Elastography for Diagnosing Mediastinal and Hilar Lymph Nodes. Chin Med J (Engl) 2015;128:2720-5.
24. Sun J, Zheng X, Mao X, Wang L, Xiong H, Herth FJF, Han B. Endobronchial Ultrasound Elastography for Evaluation of Intrathoracic Lymph Nodes: A Pilot Study. Respiration 2017;93:327-38.
25. Rozman A, Malovrh MM, Adamic K, Subic T, Kovac V, Flezar M. Endobronchial ultrasound elastography strain ratio for mediastinal lymph node diagnosis. Radiol Oncol 2015;49:334-40.
26. Nakajima T, Inage T, Sata Y, Morimoto J, Tagawa T, Suzuki H, Iwata T, Yoshida S, Nakatani Y, Yoshino I. Elastography for Predicting and Localizing Nodal Metastases during Endobronchial Ultrasound. Respiration 2015;90:499-506.
27. Ma H, An Z, Xia P, Cao J, Gao Q, Ren G, Xue X, Wang X, He Z, Hu J. Semi-quantitative Analysis of EBUS Elastography as a Feasible Approach in Diagnosing Mediastinal and Hilar Lymph Nodes of Lung Cancer Patients. Sci Rep 2018;8:3571.
28. Hernández Roca M, Pérez Pallarés J, Prieto Merino D, Valdivia Salas MDM, García Solano J, Fernández Álvarez J, Lozano Vicente D, Wasniewski S, Martínez Díaz JJ, Elías Torregrosa C, Santa Cruz Siminiani A. Diagnostic Value of Elastography and Endobronchial Ultrasound in the Study of Hilar and Mediastinal Lymph Nodes. J Bronchology Interv Pulmonol 2019;26:184-92.
29. Yong SH, Lee SH, Oh SI, Keum JS, Kim KN, Park MS, Chang YS, Kim EY. Malignant thoracic lymph node classification with deep convolutional neural networks on real-time endobronchial ultrasound (EBUS) images. Transl Lung Cancer Res 2022;11:14-23.
30. Çağlayan B, İliaz S, Bulutay P, Armutlu A, Uzel I, Öztürk AB. The role of endobronchial ultrasonography elastography for predicting malignancy. Turk Gogus Kalp Damar Cerrahisi Derg 2020;28:158-65.
31. Korrungruang P, Boonsarngsuk V. Diagnostic value of endobronchial ultrasound elastography for the differentiation of benign and malignant intrathoracic lymph nodes. Respirology 2017;22:972-7.
32. Fujiwara T, Nakajima T, Inage T, Sata Y, Sakairi Y, Tamura H, Wada H, Suzuki H, Chiyo M, Yoshino I. The combination of endobronchial elastography and sonographic findings during endobronchial ultrasound-guided transbronchial needle aspiration for predicting nodal metastasis. Thorac Cancer 2019;10:2000-5.
33. Trosini-Désert V, Jeny F, Maksud P, Giron A, Degos V, Similowski T. Contribution of endobronchial ultrasound elastography to the characterization of mediastinal lymphadenopathy: A single-center, prospective, observational study. Respir Med Res 2019;76:28-33.
34. Uchimura K, Yamasaki K, Sasada S, Hara S, Ikushima I, Chiba Y, Tachiwada T, Kawanami T, Yatera K. Quantitative analysis of endobronchial ultrasound elastography in computed tomography-negative mediastinal and hilar lymph nodes. Thorac Cancer 2020;11:2590-9.
35. Zhi X, Sun X, Chen J, Wang L, Ye L, Li Y, Xie W, Sun J. Combination of (18)F-FDG PET/CT and convex probe endobronchial ultrasound elastography for intrathoracic

malignant and benign lymph nodes prediction. Front Oncol 2022;12:908265.
36. Verhoeven RLJ, Trisolini R, Leoncini F, Candoli P, Bezzi M, Messi A, Krasnik M, de Korte CL, Annema JT, van der Heijden EHFM. Predictive Value of Endobronchial Ultrasound Strain Elastography in Mediastinal Lymph Node Staging: The E-Predict Multicenter Study Results. Respiration 2020;99:484-92.

Cite this article as: Wang Y, Zhao Z, Zhu M, Zhu Q, Yang Z, Chen L. Diagnostic value of endobronchial ultrasound elastography in differentiating between benign and malignant hilar and mediastinal lymph nodes: a retrospective study. Quant Imaging Med Surg 2023;13(7):4648-4662. doi: 10.21037/qims-23-241